Title

ASLPrep: a platform for processing of arterial spin labeled MRI and quantification of regional brain perfusion

Journal

Nature Methods, 19(6)

ISSN

1548-7091

Authors

Adebimpe, Azeez
Bertolero, Maxwell
Dolui, Sudipto
et al.

Publication Date

2022-06-01

DOI

10.1038/s41592-022-01458-7

Peer reviewed

Published in final edited form as:

Nat Methods. 2022 June ; 19(6): 683–686. doi:10.1038/s41592-022-01458-7.

ASLPrep: a platform for processing of arterial spin labeled MRI and quantification of regional brain perfusion

Azeez Adebimpe[1,2], **Maxwell Bertolero**[1,2], **Sudipto Dolui**[3], **Matthew Cieslak**[1,2], **Kristin Murtha**[1,2], **Erica B. Baller**[1,2,4], **Bradley Boeve**[5], **Adam Boxer**[6], **Ellyn R. Butler**[2], **Phil Cook**[7], **Stan Colcombe**[8,9], **Sydney Covitz**[1,2], **Christos Davatzikos**[10], **Diego G. Davila**[1,2], **Mark A. Elliott**[3], **Matthew W. Flounders**[2,11], **Alexandre R. Franco**[8,9], **Raquel E. Gur**[2,4], **Ruben C. Gur**[2,4], **Basma Jaber**[1,2], **Corey McMillian**[12],
the ALLFTD Consortium,
Michael Milham[8,9], **Henk J. M. M. Mutsaerts**[13], **Desmond J. Oathes**[2,11,14], **Christopher A. Olm**[12], **Jeffrey S. Phillips**[12], **Will Tackett**[3], **David R. Roalf**[2,4], **Howard Rosen**[6], **Tinashe M. Tapera**[1,2], **M. Dylan Tisdall**[3], **Dale Zhou**[1], **Oscar Esteban**[15,16], **Russell A. Poldrack**[16], **John A. Detre**[3,17], **Theodore D. Satterthwaite**[1,2,4,*]

[1]Penn Lifespan Informatics and Neuroimaging Center, Department of Psychiatry, Perelman School of Medicine, University of Pennsylvania, Philadelphia, PA, USA.

[2]Department of Psychiatry, Perelman School of Medicine, University of Pennsylvania, Philadelphia, PA, USA.

[3]Department of Radiology, Perelman School of Medicine, University of Pennsylvania, Philadelphia, PA, USA.

[4]Lifespan Brain Institute, Children's Hospital of Philadelphia, Philadelphia, PA, USA.

[5]Department of Neurology, Mayo Clinic, Rochester, MN, USA.

[6]Department of Neurology, University of California, San Francisco, CA, USA.

[7]Penn Image Computing and Science Laboratory, Perelman School of Medicine, University of Pennsylvania, Philadelphia, PA, USA.

[*]Please direct correspondence to: **Correspondence and requests for materials** should be addressed to Theodore D. Satterthwaite. sattertt@pennmedicine.upenn.edu.

Author contributions

A.A., M.B., S.D., M.C., K.M., E.R.B., P.C., S. Covitz., D.G.D., M.A.E., M.W.F., B.J., C.A.O., W.T., T.M.T., O.E., R.A.P., J.A.D. and T.D.S. developed ASLPrep including code, testing and documentation. A.A., M.B., M.C., K.M., D.G.D., M.A.E., S. Colcombe., C.D., M.A., B.B., A.B., A.R.F., R.E.G., R.C.G., C. McMillan., the ALLFTD Consortium, L.A., B.A., S.B., B.B., Y.B., H.B., A.L.B., A.B., D.B., D.C., G.C., R.D., D.D., K.D., K.F., A.F., J.F., T.F., L.K.F., D.G., J.G., D.R.G., R.G., T.G., J.G., N.G., I.G., M.G., M.H., E.H., H.H., G.H., E.H., D.I., D.T.J., K.K., D. Kaufer, D. Kerwin, D. Knopman, J. Kornak, J. Kramer, W.K., M.L., A.L.L., G.L., P.L., I.L., D.L., I.M., J.C.M., S.M., M. Mendez,. C. Mester, B.L.M., C.O., M.B.P., L.P., P.P., R.P., V.R., E.M.R., M.R., K.R., K.P.R., A.R., E.D.R., J.R., H.J.R., R.S., W.S., J.S., A.M.S., M.C.T., J.T., L.V., S.W., B.W., Z.W., M. Milham., D.J.O., J.S.P., D.R.R., H.R., M.D.T., D.Z. and T.D.S. contributed and curated data. A.A., M.B., S.D., M.C.,
D.Z. and T.D.S. processed and analyzed the data. A.A., M.B., S.D., M.C., K.M.,E.B.B., B.B., A.B., E.R.B., P.C., S. Colcombe, S. Covitz., C.D., M.A.E., D.G.D., M.A.E., M.W.F., A.R.F., R.E.G., R.C.G., B.J., C. McMillan, L.A., B.A., S.B., Y.B., H.B., A.L.B., A.B., D.B., D.C., G.C., R.D., D.D., K.D., K.F., A.F., J.F., T.F., L.K.F., D.G., J.G., D.R.G., R.G., T.G., J.G., N.G., I.G., M.G., M.H., E.H., H.H., G.H., E.H., D.I., D.T.J., K.K., D. Kaufer, D. Kerwin,D. Knopman, J. Kornak, J. Kramer, W.K., M.L., A.L.L., G.L., P.L., I.L., D.L., I.M., J.C.M., S.M., M.Mendez,. C.Mester, B.L.M., C.O., M.B.P., L.P., P.P., R.P., V.R., E.M.R., M.R., K.R., K.P.R., A.R., E.D.R., J.R., H.J.R., R.S., W.S., J.S., A.M.S., M.C.T., J.T., L.V., S.W., B.W., Z.W., M. Milham, H.J.M.M.M., D.J.O., C.A.O., J.S.P., W.T., D.R.R., H.R., T.M.T., M.D.T., D.Z., O.E., R.A.P., J.A.D. and T.D.S. assisted with writing and editing the manuscript.

Competing interests

The authors declare no competing interests.

[8]Child Mind Institute, New York, NY, USA.

[9]Center for Brain Imaging and Neuromodulation, Nathan S. Kline Institute for Psychiatric Research, Orangeburg, NY, USA.

[10]Center for Biomedical Image Computing and Analytics, Perelman School of Medicine, University of Pennsylvania, Philadelphia, PA, USA.

[11]Center for Neuromodulation in Depression and Stress, Perelman School of Medicine, University of Pennsylvania, Philadelphia, PA, USA.

[12]Frontotemporal Degeneration Center, Perelman School of Medicine, University of Pennsylvania, Philadelphia, PA, USA.

[13]Department of Radiology and Nuclear Medicine, Amsterdam University Medical Center, Amsterdam Neuroscience, Amsterdam, the Netherlands.

[14]Penn Brain Science, Translation, Innovation, and Modulation Center, Perelman School of Medicine, University of Pennsylvania, Philadelphia, PA, USA.

[15]Department of Radiology, Lausanne University Hospital and University of Lausanne, Lausanne, Switzerland.

[16]Department of Psychology, Stanford University, Stanford, CA, USA.

[17]Department of Neurology, Perelman School of Medicine, University of Pennsylvania, Philadelphia, PA, USA.

Arterial spin labeled (ASL) magnetic resonance imaging (MRI) is the primary method for noninvasively measuring regional brain perfusion in humans. We introduce ASLPrep, a suite of software pipelines that ensure the reproducible and generalizable processing of ASL MRI data. Despite comprising only 2% of human body mass, the adult brain receives approximately 15% of cardiac output to support the intensive demands of neural computation[1]. Cerebral blood flow (CBF) is tightly linked to brain metabolism[2], varies predictably across the lifespan[3] and is increasingly seen as an important biomarker of diverse neuropsychiatric and neurological disorders[4]. Although the gold standard method of measuring CBF is 15O-positron emission tomography (PET), arterial spin labeled (ASL) perfusion magnetic resonance imaging (MRI) has evolved to become the dominant method for noninvasive, contrast-free measurement of CBF in humans due to its ease of implementation and lack of either injected contrast or ionizing radiation[5].

The ascendancy of ASL MRI has also been accompanied by a rapid rise of both acquisition methods and analytic techniques[5]. For example, widely used ASL MRI sequences vary in their labeling type, number of echo times, labeling duration, number of post-labeling delays (PLDs) used, image scaling, background suppression and the acquisition of a reference (M0) image. Furthermore, different MRI schemes for ASL may yield markedly different outputs: commonly used schemes can provide a timeseries of control and label pairs, a single difference image or a fully quantified CBF image. When combined, these factors have limited the generalizability of techniques for the processing and quantification of CBF and have slowed the pace of translational research[6]. To address this gap, we introduce ASLPrep:

a generalizable and robust software workflow that allows for reproducible processing of a wide range of ASL MRI data (Fig. 1).

ASLPrep requires imaging metadata be recorded in brain imaging directory structure (BIDS)[7] format and leverages BIDS to automatically configure appropriate workflows based on the data provided. ASLPrep was inspired by fMRIPrep[8], which provides adaptive and reliable processing of fMRI data but does not provide functionality for the processing of ASL images or quantification of CBF. ASLPrep builds on widely used neuroimaging toolboxes, such as FSL[9], FreeSurfer[10], AFNI[11], ANTs[12] and diverse Python packages (Supplementary Tables 1 and 2); like fMRIPrep, ASLPrep depends on sMRIPrep[13] for structural processing and SDCFlows[14] for distortion correction. ASLPrep also includes in-house implementations for algorithms unavailable elsewhere, for instance the structural correlation based outlier rejection (SCORE) denoising option[15], which is useful for studies of populations with greater head motion, such as children and many clinical populations.

Building on this preprocessing workflow, ASLPrep can execute advanced methods to quantify CBF. In addition to the standard CBF quantification procedure that uses a general kinetic model[16], ASLPrep includes two different Bayesian models that incorporate information regarding brain structure: BASIL (Bayesian inference for arterial spin labeling)[17] and SCRUB (structural correlation with robust Bayesian)[18]. Following computation of the CBF map, BASIL also provides partial volume corrected (PVC) gray matter (GM) and white matter (WM) perfusion maps, which adjusts CBF according to the mixture of GM and WM present in the anatomical image. For all quantification models, regional CBF can be summarized in a diverse set of standard atlases or custom atlases provided by the user.

By refactoring the reporting system of fMRIPrep[8] to be compatible with ASL data, both minimal preprocessing and quantification workflows are transparently documented with a detailed visual report that is generated dynamically. Each step in the workflow is demonstrated and its performance can be assessed for quality with dedicated visualizations (Supplementary Fig. 1). In addition to such visualizations, ASLPrep provides multiple quantitative measures of image quality. Like fMRIPrep[8], processing reports also include a ‘citation boilerplate’ that comprehensively describes the actual workflow implemented, including software versions and relevant citations to facilitate maximally transparent reporting in papers that use ASLPrep.

ASLPrep is distributed as a Docker image that includes all dependencies (https://hub.docker.com/r/pennlinc/aslprep), ensuring that it can be run in nearly any computing environment. The modular code base of ASLPrep uses Nipype[19] and is openly developed on GitHub (https://github.com/pennlinc/aslprep), allowing for rapid detection of bugs, integration of feature requests and support for the international user base. Before the release of patches or new versions, all changes to the underlying code of ASLPrep are subject to continuous integration testing via CircleCI. Extensive documentation (https://aslprep.readthedocs.io) is version controlled and frequently updated, facilitating broad dissemination. So far, a total of more than 48,000 datasets have been successfully processed using ASLPrep by users worldwide.

To illustrate the generalizability of ASLPrep, we processed five different datasets acquired with a wide range of acquisition parameters (n=3,571 total scans, 1,978 females, mean age of 26.88years, s.d.=19.79years, Supplementary Table 3). These datasets included four ASL sequences collected on Siemens scanners using pseudo-continuous labeling (PCASL), but different encoding schemes: two-dimensional (2D) spin-echo PCASL images from the Philadelphia Neurodevelopmental Cohort (PNC) (n=1,527, 797 females, mean age 15.00years, s.d.=3.65 years), 2D gradient echo-images from the NKI-Rockland sample (NKI) (n=1,648, 956 females, mean age 36.35years, s.d.=22.66 years), a three-dimensional (3D) stack-of-spirals spin-echo acquisition from a study of irritability in youth (IRR) (n=218, 136 females, mean age of 21.56 years, s.d. = 3.51 years) and a publicly available study of aging that used a 3D GRASE PCASL sequence (AGE) (n = 63, 35 females, mean age of 48.98years, s.d.=24.41 years). Furthermore, we included a study of fronto-temporal dementia (FTD) (n=115, 54 females, mean age of 53.47 years, s.d. = 15.36 years) that was collected on a GE scanner using a 3D EPI gradient echo sequence with PCASL. For each of these diverse datasets, we completed both minimal preprocessing and CBF quantification. Specifically, we evaluated the mean CBF of GM and WM in each dataset, and examined how GM CBF evolved with age[20]. While these analyses focused on CBF quantified using the standard CBF quantification procedure, we also conducted analyses using the other quantification methods packaged with ASLPrep.

Across datasets and workflows, pipelines automatically configured by ASLPrep finished without errors. As part of quality assurance, 5% participants with gross motion (frame-wise displacement greater than 1 mm) or nonphysiologic CBF (for example, a ratio of GM to WM CBF of less than 1) were excluded from further analyses (Supplementary Table 4; final sample n = 3,383). Inspection of data from individual participants (Extended Data Fig. 1) as well as group average CBF from each dataset (Extended Data Fig. 2) revealed a consistent performance. Compared to a pipeline previously used in published studies of the PNC, ASLPrep preserved anatomical detail and reduced blurring (Extended Data Fig. 3). Furthermore, there was good alignment between the regional distribution of CBF quantified using ASLPrep and a commonly used PET atlas (Extended Data Fig. 4). When we evaluated the impact of in-scanner motion on data quality across quantification methods, Bayesian methods (such as BASIL) attenuated the impact of participant movement (Extended Data Fig. 5). As expected, the distinction between GM and WM CBF was more striking in datasets of youth and was reduced in datasets that were composed of older individuals (Fig. 2a and Extended Data Fig. 6). When we aggregated data from individual participants across all datasets, the anticipated nonlinear decline of CBF over the lifespan was evident (Fig. 2b). While GM atrophy in aging may produce a decline in CBF due to partial volume effects, a nonlinear decline in CBF was still apparent after partial volume correction ( ).

Across the over 3,000 participants evaluated, the processing time of ASL images using ASLPrep did not exceed 70 minutes (when executed using four cores and 30GB of RAM). However, ASLPrep also requires anatomical image processing, which increases the total runtime of ASLPrep to a mean of 4.5hours (Extended Data Fig. 8). However, one critical feature of ASLPrep is that it can consume processed anatomical images that conform to the BIDS-derivatives standard (for example, sMRIPrep[13]) obviating the need for reprocessing structural images and accelerating runtime. This feature is particularly important for multi-

modal imaging studies, as it allows a single source of preprocessed anatomical information to be used, ensuring consistency across image types (ASL, fMRI, dMRI, etc).

In summary, ASLPrep allows investigators to correctly apply reproducible preprocessing pipelines and advanced CBF quantification methods to ASL images that conform to the BIDS standard ASLPrep adapts its workflow to the characteristics of the input data, ensuring appropriate image processing if the data have been correctly specified in BIDS. By harnessing complementary techniques from multiple software packages and combining them in an interoperable framework, ASLPrep reduces the burden on investigators who wish to avoid learning the details of many disparate techniques. Taken together, ASLPrep ensures fully reproducible and widely generalizable processing, quality assurance and quantification of ASL images.

Online content

Any methods, additional references, Nature Research reporting summaries, source data, extended data, supplementary information, acknowledgements, peer review information; details of author contributions and competing interests; and statements of data and code availability are available at https://doi.org/10.1038/s41592-022-01458-7.

Methods

ASLPrep allows investigators to easily process diverse ASL MRI[5,21] data and compute CBF. ASLPrep is designed using an adaptive architecture that leverages the Brain Imaging Data Structure (BIDS)[7], an open standard for describing neuroimaging data. ASLPrep reads the metadata provided by BIDS, allowing workflows to automatically adapt to the parameters of the data without manual intervention. ASLPrep leverages Nipype[19] to ensure compatibility across tools from many software packages (for example, Freesurfer, AFNI, ANTS, FSL) and effectively combine their complementary strengths (Supplementary Table 1).

ASLPrep's design is inspired by fMRIPrep[8] and adheres to the principles of NiPreps[22] (www.nipreps.org): it maximizes interoperability and adaptability to input data with BIDS, it reproducibly delivers 'analysis-ready' data so that researchers can confidently focus on statistical modeling, and code is managed with software engineering techniques to ensure quality and reliability following BIDS-Apps' directions[23] (for example, uses open-source development, implements version control with GitHub, includes continuous integration of testing with CircleCI to check every code update and so on). ASLPrep is composed of four main workflows (Fig. 1): anatomical preprocessing, ASL preprocessing, CBF computation and assessment of image quality.

Anatomical preprocessing.

The anatomical preprocessing workflow in ASLPrep leverages sMRIPrep (v.0.6.1)[13], a structural MRI (sMRI) processing pipeline. sMRIPrep performs basic processing steps including subject-wise averaging, bias field correction, segmentation and spatial normalization. The anatomical outputs of sMRIPrep can be used while processing multi-modal imaging data, including fMRIPrep[8], QSIPrep[24] and ASLPrep. The main steps of anatomical preprocessing are summarized below:

Bias field correction and T1w subject-wise averaging.—The structural T1w image is first corrected for intensity nonuniformity with N4BiasFieldCorrrection[25] as implemented in ANTs. If there are several T1w images, bias-corrected corrected images are fused into a reference T1w map with Freesurfer's mri_robust_template[26].

Brain extraction and tissue segmentation.—The bias-corrected T1w image is skull-stripped with antsBrainExtraction.sh using either the OASIS[27] (default) or NKI[28] template. Note that the template used here for brain extraction is distinct from the template used for spatial normalization. After brain extraction, FSL's FAST[29] is used to segment the T1w brain into cerebrospinal fluid (CSF), GM and WM. FAST produces both a hard segmentation as well as partial volume estimates for each tissue class.

Spatial normalization and template selection.—Following bias correction and brain extraction, the T1w image is normalized to the MNI152 Nonlinear Asymmetric[30,31] template using the top-performing deformation provided by antsRegistration[32]. Beyond the MNI template, Templateflow[31] allows for the selection of other available templates including the PNC[33], NKI and OASIS templates.

ASL preprocessing.

Due to the variety of ASL data types, ASL preprocessing workflows require that the input data conform to the ASL BIDS specification. The processing workflows can accommodate disparate ASL labeling approaches[5], readout methods[34] and number of volumes in the ASL input data. The most common labeling approaches include continuous labeling, pulsed labeling and PCASL, with PCASL the method recommended in a recent consensus white paper[5].

Input data.—The four possible types of ASL data provided by an acquisition sequence are: (1) a timeseries of control and label images, (2) a ΔM image, (3) an M0 image and (4) a quantified CBF image. It should be noted that the ΔM and CBF images are derived rather than raw data. However, some ASL sequences from GE or Philips scanners provide these derived images instead of the raw ASL timeseries; as such they are considered as potential input data to ASLPrep. These possible inputs are briefly defined below:

1. ASL timeseries: a typical ASL timeseries consists of control and label images, which are acquired in pairs in an ASL sequence, and scaled identically. When background suppression is not used, the control image can be used in place of the M0 image for calibration. Most but not all ASL sequences will provide this timeseries; some sequences will provide an ΔM image or the fully quantified CBF image.
2. ΔM: the ΔM images are formed by the pairwise subtraction of the label and control images. Multiple control-label pairs are always acquired, which after subtraction generates a timeseries of ΔM images. Some sequences provide an average ΔM image rather than the full ASL timeseries of control and label pairs; ASLPrep can recognize and process either.

3. M0: an M0 image is used as a reference image and to estimate the equilibrium magnetization (M0) of blood. If an M0 scan is not provided, the average of the control images is used as the reference (while checking for background suppression). Alternatively, a user-specified M0 value specified in the BIDS metadata will override the M0 scan (if present) and be used for calibration.

4. CBF: the quantified CBF image is produced by dividing the ΔM by the processed M0 image or by the user-specified M0 value specified in BIDS. Using a standard model, the CBF image is then scaled into physiological units (ml per 100 g min−1). Rarely, ASL sequences provide a fully quantified CBF map instead of an ASL timeseries or a ΔM image. In this case, most steps of ASLPrep are obviated. However, normalization to a template and calculation of average values for atlas parcels can still be performed. In this case, an M0 image is necessary for generation of a high-quality brain mask.

Using this input data, the general ASL preprocessing workflow is as follows:

Reference volume selection.—For each ASL dataset, a reference volume for motion correction and co-registration is selected. When an ASL timeseries is provided, the median of ASL volumes is selected as the reference volume. For a single ΔM or CBF image, the M0 scan (if present) is used as the reference volume. The reference volume is skull-stripped with FSL's BET[35] and refined with the co-registered T1w brain mask.

Motion estimation.—The head motion parameters from the ASL timeseries (if available) are estimated with FSL's MCFLIRT[36].

Slice-timing correction.—If slice-timing information is available in the metadata,the slice-timing correction is performed on the ASL data with AFNI's[11] 3dTshift. However, slice-timing correction is optional, can be turned off and is not applied if slice times are not specified in the BIDS metadata. Note that while slice-timing correction can be applied for 2D ASL data, it is not recommended for 3D ASL data.

ASL-T1w coregistration.—Coregistration aligns the T1w image and ASL reference volume. This uses boundary-based coregistration as implemented with FSL's FLIRT[37]. A rigid body transform (six degrees of freedom) is specified by default. Forward and backward transformation matrices are generated for required subsequent preprocessing.

Distortion correction.—Distortion correction is implemented using SDCFlows[38] (susceptibility distortion correction workflows). SDCFlows provides workflows for the preprocessing of several MRI schemes that allow the estimation of B0 field-inhomogeneity maps, which are directly related to the distortion. Distortion correction is applied to the ASL data if the appropriate fieldmap information is provided in the BIDS metadata. Distortion correction is optional. SDCFlows additionally includes an experimental fieldmap-less[39] distortion correction method, which uses a nonlinear registration between the ASL reference image and the T1w image.

CBF computation.

Following common preprocessing steps, there are two streams for CBF computation and denoising. The first stream is the default (Basic CBF) and consists of CBF computation with the general kinetic model[16,40]. The first step produces a CBF timeseries if there are multiple control-label pairs or ΔM images provided. Optionally, this CBF timeseries can then be denoised using SCORE[15]. Last and also optionally, a Bayesian model can be applied that incorporates data from the anatomic image using SCRUB[18].

The second stream uses FSL's BASIL toolbox. BASIL's Bayesian model incorporates spatial regularization and produces a single CBF map. Note that because it produces a single CBF map rather than a CBF timeseries, it cannot be used jointly with SCORE. Following computation of the CBF map, BASIL also calculates a GM and WM CBF map with partial volume correction applied.

Both common steps and specific procedures for each of the two CBF computation streams are detailed below:

Procedures common to both processing streams.—ΔM Computation: after ASL preprocessing, the ΔM images are extracted. Depending on the ASL input data, the label and controls images are subtracted pairwise to obtain a timeseries of ΔM images. However, if input data contain a ΔM image or CBF maps, this step is not performed.

CBF calibration: as noted above, the ΔM images require scaling to calculate CBF. This can be done using a dedicated M0 image (preferred), the average of the control images from the ASL timeseries (if no background suppression is used) or a user-specified value provided in the JSON. If an M0 image is present, it will be used instead of the mean of the control images. However, specification of an M0 value in the JSON will force its application regardless of the other images present; this should generally be avoided. Default smoothing of M0 scan images is implemented with 5 mm full-width at half-maximum, but the users can adjust to any value. Smoothing of the M0 is advisable for CBF computation.

Stream 1: standard CBF ± SCORE and SCRUB.—CBF quantification with the standard model: CBF is quantified based on the general kinetic model[16,40] and requires several parameters[5], including labeling duration, PLD, T1-blood relaxation time, labeling efficiency, blood–brain partition coefficient and inversion time. Some of these parameters (such as bolus duration, labeling duration and PLD) are specific to the ASL labeling techniques. The other parameters (such as labeling efficiency and blood–brain partition coefficient) depend on the labeling approaches (PCASL or pulsed labeling) and hardware (for example, MRI machine magnetic strength). ASLPrep quantifies CBF for both single delay (one PLD) and multi-delay (multiple PLDs) ASL data. The multi-delay ASL data give us the opportunity to estimate arterial transit time using signal weighted delay[41]. All parameters necessary for computation of CBF using the standard model are read from the JSON that adheres to the BIDS specification for ASL.

CBF denoising with SCORE: CBF is known to be susceptible to artifacts[42] especially from head motion. ASL's low signal to noise ratio (SNR), particularly when acquired

without background suppression, is compensated for by averaging multiple label-control pairs. However, some volumes may be corrupted and can influence the average of the CBF map. The corrupted volumes are likely to be outliers of the CBF timeseries. To identify and remove these outlier volumes, ASLPrep implements SCORE[15]. The first step of SCORE is the detection of a small number of extreme outliers before further processing. These outliers are identified as CBF volumes with mean CBF in GM tissue that is greater than 2.5 times the standard deviation of the mean GM CBF. In the second step, each remaining CBF volume is compared to average CBF maps to detect noise in these volumes. The variability of CBF values in the three tissue types, GM, WM and CSF, is calculated. Then, CBF volumes with high variance of CBF values in the three anatomical tissues are flagged as outliers. In each step, outliers are identified and the remaining CBF volumes are averaged. The variance of averaged CBF in the three anatomical tissue classes is then compared with the previous iteration. The procedure is repeated while the CBF variance in anatomical tissues is lower than those previous iterations. In the last iteration, all outlier volumes are discarded before averaging the remaining CBF volumes. For further details, see ref.[15]

Bayesian estimation of CBF with SCRUB: while SCORE detects and removes outlier volumes that contribute to spatially constrained artifacts, Bayesian techniques may be used to improve SNR. Accordingly, ASLPrep optionally allows users to implement SCRUB[18]. SCRUB incorporates information from the structural image as a prior in a Bayesian to reduce noise and improve SNR. SCRUB uses an iterative reweighted least square method to estimate CBF inside a Bayesian framework. In this framework, the reweighted CBF at each voxel is comparedto the prior provided by a standard CBF based on the tissue probability maps from the soft segmentation of the anatomic image. A reliable CBF map is more likely when the CBF temporal variance is less than the mean CBF variance. If the CBF temporal variance is greater than the mean CBF variance, a higher weight is assigned to the previous term. For further details regarding SCRUB, see ref.[18].

Stream 2: CBF computation with BASIL ± partial volume correction.—CBF computation with BASIL: ASLPrep includes the ability to compute CBF using BASIL[17]. BASIL was originally developed for CBF computation of multi-PLDs data, but it also can be used with single PLD data. BASIL uses a fast Bayesian inference method for the kinetic model inversion and includes perfusion estimation and associated variables, such as arterial transit time. BASIL also allows for the inclusion of the variability of other model parameters, such as relaxation timesfor tissue and blood, as well as labeling durations. After CBF computation, BASIL applies a Gaussian process based before computed CBF maps for adaptive spatial regularization[43]. For further details regarding BASIL, see ref.[17].

Partial volume correction with BASIL: the low spatial resolution is a limitation of ASL and leads to partial volume effects[5]. Partial volume effects occur when voxels near the boundary between different tissue types (for example, GM and WM) contain a mixture of the respective tissues. As a result, a given voxel may have apparently lower CBF due to the greater proportion of WM at that location. Partial volume effects are particularly relevant in ASL data, where the ASL signal intensity at each voxel represents mixtures of signals from GM and WM (CSF perfusion is assumed to be zero). Partial volume effects can be accounted for using partial volume correction. High-resolution GM and WM probability

maps from T1 segmentation are transformed into the low-resolution space of the ASL data, allowing the relative mix of GM and WM at each ASL voxel to be estimated. BASIL uses these data in conjunction with adaptive spatial regularization to yield PVC CBF maps for both GM and WM. For further details, see ref.[44].

Measures for quality control.

ASLPrep generates a rich set of indices to assist in the quality control process. Because many errors of image processing result from problems with image registration, ASLPrep calculates measures that assess the quality of both co-registration of the ASL to the T1w image, as well as normalization of the T1w image to the specified template. Specifically, ASLPrep calculates the mask overlap, spatial correlation, Dice coefficient and Jaccard index for each step of registration. Furthermore, ASLPrep provides several quality measures for the ASL timeseries, including the mean frame-wise displacement[45], the root mean square variance of temporal derivative of CBF time courses (DVARS)[46], the number of voxels with a negative CBF and the CBF quality evaluation index (QEI)[47]. QEI is a quantitative metric of the quality of CBF maps based on the CBF map's similarity with the structural tissues, the CBF spatial variability in each tissue class (GM, WM) and the percentage of negative voxels in the GM mask. QEI ranges from 0 from 1, with higher values referring to higher quality CBF maps; previous work has established that it is an excellent proxy of CBF image quality[47]. Finally, ASLPrep calculates the ratio of CBF in the GM mask to CBF in the WM mask; this ratio is expected to be greater than 1. All quality indices described above are written to a text file (tab-separated values) for each session processed; these are easily concatenated across participants to facilitate rapid quality assurance of large-scale ASL studies.

Regional quantification.

As a final step, ASLPrep optionally quantifies the mean CBF in each parcel in each of the standard atlases. To do this, standard atlases are transformed to CBF native space using a single interpolation. The mean of CBF values of each atlas's parcels is extracted into a comma-separated values (.csv) file. At present, the Harvard–Oxford[48] and Schaefer[49] (200 and 400 parcel resolution) atlases[50] are included.

Standard output.

Processed data are named and include metadata to conform to the proposed BIDS specification for derived data.

The anatomical derivatives generated by sMRIPrep are placed in each participant's anat/ subfolder. The main derivatives, in T1w and template spaces, include:

1. Preprocessed T1w, brain mask and tissues segmentation mask
2. GM, WM and CSF partial volume estimates
3. Transformation files for normalization between the T1w image and the template

ASL derivatives: similarly, ASL derivatives are stored in the perf/ subfolder. Based on the anatomical preprocessing, users can specify one or more output spaces: native ASL,

T1w, and one or more standard templates (MNI, OASIS, PNC and others, as available on TemplateFlow[31]) MNI output space is the default, which is written out in the resolution of the original ASL image. However, users can specify as many output spaces as they want. The main output in any space includes:

- ASL reference volume, brain mask and preprocessed data
- CBF timeseries and mean CBF map
- Transformation files or transforms between T1w and ASL reference
- Arterial transit time image, if multiple PLDs are available
- SCORE and/or SCRUB CBF maps, if requested
- BASIL and/or PVC CBF maps, if requested
- Quality control measures summarized in a .TSV file. The quality control measures include mean frame-wise displacement, relative root mean square of motion parameters (relRMS), DVARS, registration and normalization indexes, mean CBF, ratio of CBFGM to CBFWM and QEI for each CBF map.
- Regional quantification of CBF according to specified atlases written in a .CSV file
- Confound matrix for each ASL volume in a .TSV file. The confound matrix includes six motion parameters, frame-wise displacement and DVARS for each processed ASL volume.

ASLPrep report.

ASLPrep generates a descriptive HTML report for each participant and session (Supplementary Fig. 1). The report begins with a summary of key parameters found by ASLPrep in the BIDS layout. Subsequently, it lists the key operations and processing steps applied to the dataset. Notably, each step includes a thorough visual assessment of the data, including ‘before’ versus ‘after’ animations of each step. These visualizations include normalization, coregistration and distortion correction. The report additionally includes a carpet plot of both the raw and processed image timeseries, as well as views of all CBF maps generated. The report details multiple quality control features, including in-scanner motion, QEI, coregistration and normalization quality (overlap of coverage, Dice coefficient, Jaccard index) and mean CBF in both GM and WM masks. Critically, the report ends with boilerplate methods text, which provide a clear and consistent description of all preprocessing steps used, provided with appropriate citations.

Application of ASLPrep to lifespan data.

Datasets and ASLPrep execution.—The general workflow (Fig. 1) was applied to datasets with diverse participant populations and scanning parameters. No new data were collected specifically for this study; all data were acquired with Institutional Review Board approval at their original institutions. The University of Pennsylvania Institutional Review Board approved the PNC, FTD and IRR studies. The AGE and NKI datasets are publicly available, deidentified data resources. Supplementary Table 3 describes the acquisition

parameters of the datasets used; Supplementary Table 4 details the main preprocessing operations that were automatically applied to each dataset. One dataset included both an ASL timeseries of control-label pairs as well as an M0 image (IRR). In contrast, three datasets had control-label timeseriesbut lacked an M0 image (NKI, PNC, AGE), and one dataset only included ΔM and M0 images (FTD). Furthermore, the acquisition types of these datasets were also different: PNC and NKI were acquired in 2D while the other datasets were acquired in 3D. All data were collected using 3 T scanners. For each study, CBF was quantified using four approaches: the standard CBF model, SCRUB (with SCORE denoising turned on), BASIL and BASIL + PVC. All ASL data outputs were resampled to MNI2009a with resolution of 2 mm for uniformity. The only exception to this was the FTD dataset, where SCRUB could not be applied as it requires an ASL timeseries.

Each set of participant data was processed using ASLPrep v.0.2.7 (ref. [50]) with four cores and 30 GB of RAM on the CUBIC High-Performance Cluster at the University of Pennsylvania. Notably, the anatomical preprocessing with sMRIPrep required substantially more time than ASL processing (Extended Data Fig. 8). While anatomical preprocessing took an average of 4.5 h, the ASL processing was completed in an average of 33.5 min.

Statistical analysis

For each CBF map, the mean CBF in GM and WM masks were extracted. To do this, as suggested[51], GM and WM probability maps derived from segmentation of the T1 image were transformed into native ASL space and binarized after thresholding at 70% probability; average CBF values were calculated in this mask in native ASL space. As part of quality assurance, we excluded participants with mean frame-wise displacement greater than 1 mm or a CBF GM to WM ratio of less than 1. The quality assurance process resulted in a sample of 3,383 participants used for subsequent analysis (Supplementary Table 4). CBF in GM and WM masks were extracted for all the CBF maps (standard CBF, SCRUB, BASIL and BASIL + PVC). To rigorously model both linear and nonlinear evolution of CBF over the lifespan, the mean GM CBF was regressed on age using a generalized additive model with penalized splines.

We also evaluated the degree of anatomical detail preserved by ASLPrep in comparison to a previously published pipeline used for data from the PNC[52]. Image smoothness for each participant across each study was evaluated in template space and compared across pipelines using a two-sided paired *t*-test.

While the alignment between PET and ASL has been established in previous reports[53], we compared CBF as quantified using ASLPrep to CBF measured using PET. Specifically, CBF calculated using ASLPrep was averaged in template space across datasets and correlated with the [15O]water PET atlas included in Statistical Parametric Mapping (SPM). To account for spatial autocorrelation and nonindependence of measurements, the similarity of the images was assessed using BrainSmash[54], a conservative permutation-based testing procedure that uses generative models to preserve the spatial covariance structure in the null distribution.

Finally, to examine the impact of data quality on each quantification method, we examined the relationship between data quality (summarized by the QEI) and in-scanner motion (summarized by frame-wise displacement). This relationship was evaluated for each quantification method and each dataset. The impact of quantification method on the relationship between in-scanner motion and data quality was evaluated using a linear mixed effects model, where QEI was the outcome and frame-wise displacement, age, sex, quantification method and dataset were modeled as fixed effects, and participant was modeled as a random effect. The effect of interest was the interaction between quantification method and frame-wise displacement on QEI.

All code used to perform the statistical tests are available at https://pennlinc.github.io/aslprep_paper, under the BSD-3-Clause License.

Data availability

All quantified data are available as Source Data files provided with this paper. Additionally, raw data are available for many of the datasets used in evaluation of the software, depending on the original source of the data. PNC data are available on dbGAP (https://www.ncbi.nlm.nih.gov/projects/gap/cgi-bin/study.cgi?study_id=phs000607.v3.p2). NKI neuroimaging data are openly availableon the NeuroImaging Tools and Resources Collaboratory (https://fcon_1000.projects.nitrc.org/indi/enhanced/). AGE data are available on Open Neuro (https://openneuro.org/datasets/ds000240/versions/00002). For the remaining datasets, we do not control the distribution of them, but requested can be made to the original authors. The IRR dataset will be released publicly; at present, it is available on request from the corresponding author. Access to the FTD dataset is governed by the ALLFTD Consortium.

Code availability

ASLPrep is available under the BSD-3-clause license at https://github.com/pennlinc/aslprep. Docker images corresponding to every new release of ASLPrep are automatically generated and made available on Docker Hub (https://hub.docker.com/r/pennlinc/aslprep). All code used to perform the statistical tests are available at: https://pennlinc.github.io/aslprep_paper, under the BSD-3-Clause License. Software documentation is available at https://aslprep.readthedocs.io. ASLPrep code is also available through Zenodo: https://doi.org/10.5281/zenodo.4815777 (ref. 55) and as part of a Code Ocean compute capsule: https://doi.org/10.24433/CO.7220174.v1 (ref. 56).

Extended Data

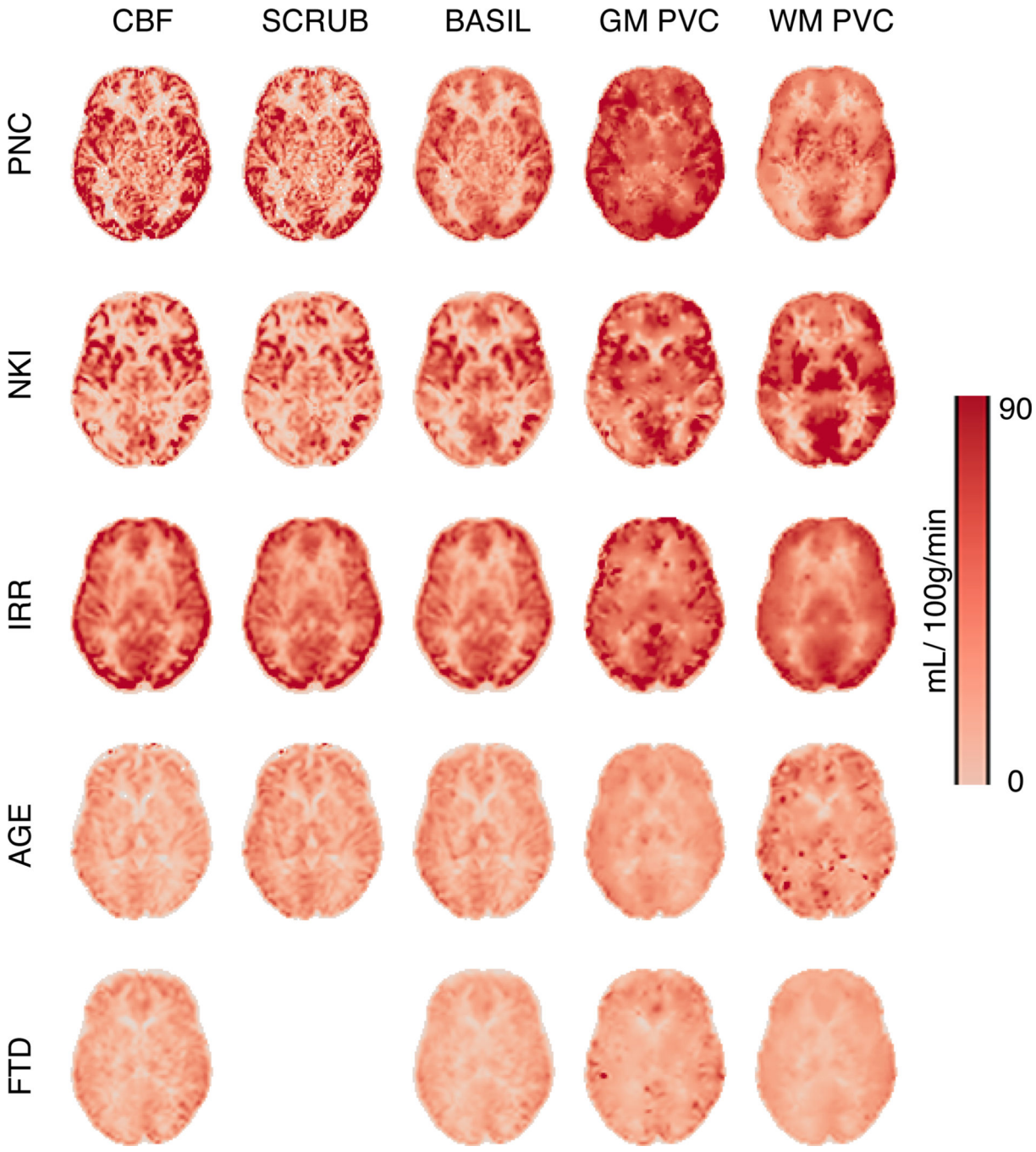

Extended Data Fig. 1. Exemplar data for each dataset and CBF quantification method.
A single participant from each dataset is shown (in MNI space), with CBF quantified using each of four methods. SCRUB could not be applied for the FTD dataset as an ASL timeseries is required; the sequence used for that study provided only a ΔM image.

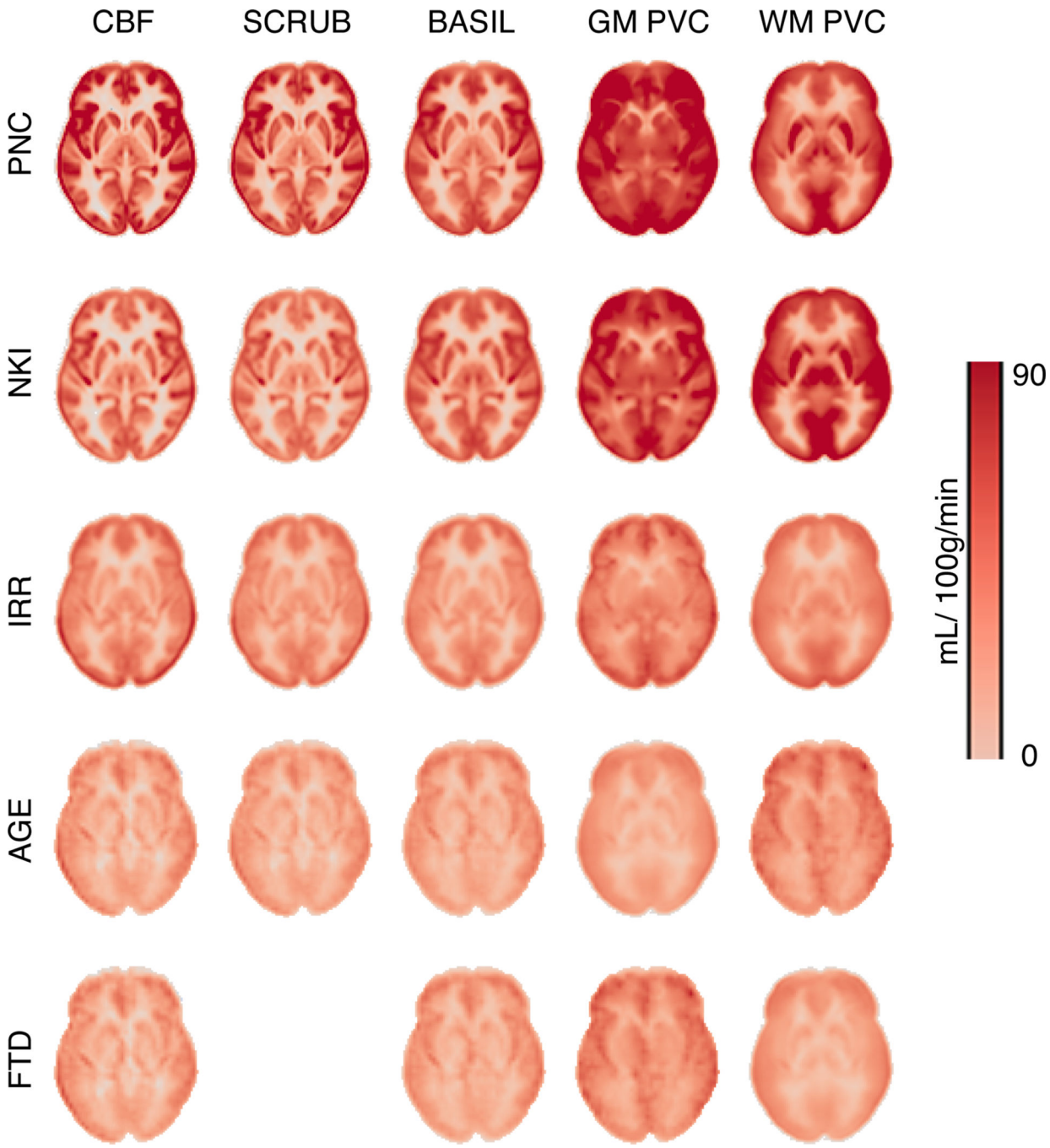

Extended Data Fig. 2. Mean cerebral blood flow maps for each dataset and quantification method.

CBF quantification for each dataset using the four methods supported by ASLPrep. An axial slice (z = 0) of the mean CBF image for each dataset is displayed (in MNI space) for each quantification method. SCRUB could not be applied for the FTD dataset as an ASL timeseries is required; the sequence used for that study provided only a single ΔM image.

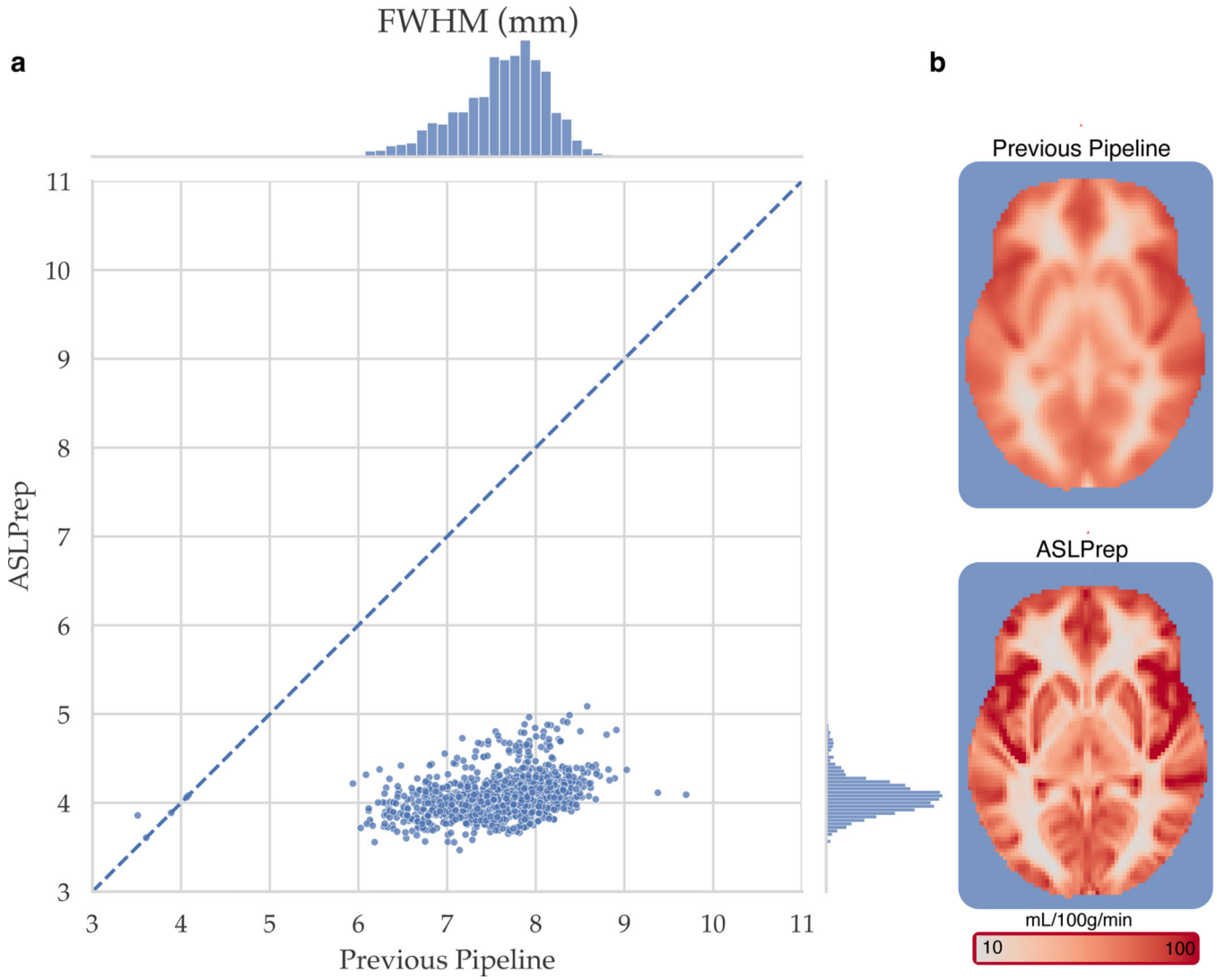

Extended Data Fig. 3. Image smoothness from a legacy pipeline and ASLPrep.

a) Comparison of CBF quantified with ASLPrep and a previously published pipeline used for the PNC; both pipelines implemented the standard kinetic model. Image smoothness in template space differed between ASLPrep and the previous pipeline (two-sided *t*-test; $t(1,480) = 252.58$, $p < 1 \times 10^{-16}$). **b**) Across-dataset average image.

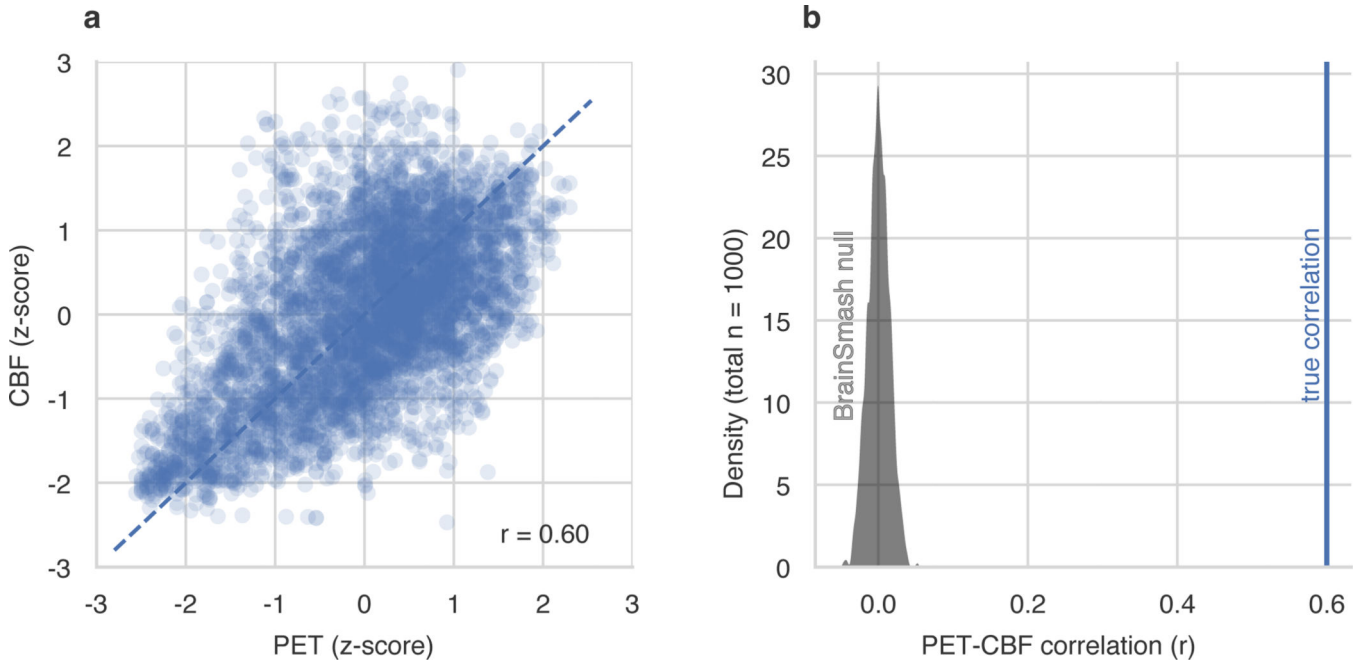

Extended Data Fig. 4. CBF quantified using ASLPrep aligns with a commonly used PET atlas.
a) CBF quantified using ASLPrep (averaged across datasets) aligned with CBF from a commonly used PET atlas included in SPM, where CBF was measured using [^{15}O]water PET (Pearson $r = 0.60$). **b**) Assessment of the similarity of the images using a null distribution (comparison with a Brainsmash null $p = 0.0001$; panel **b**).

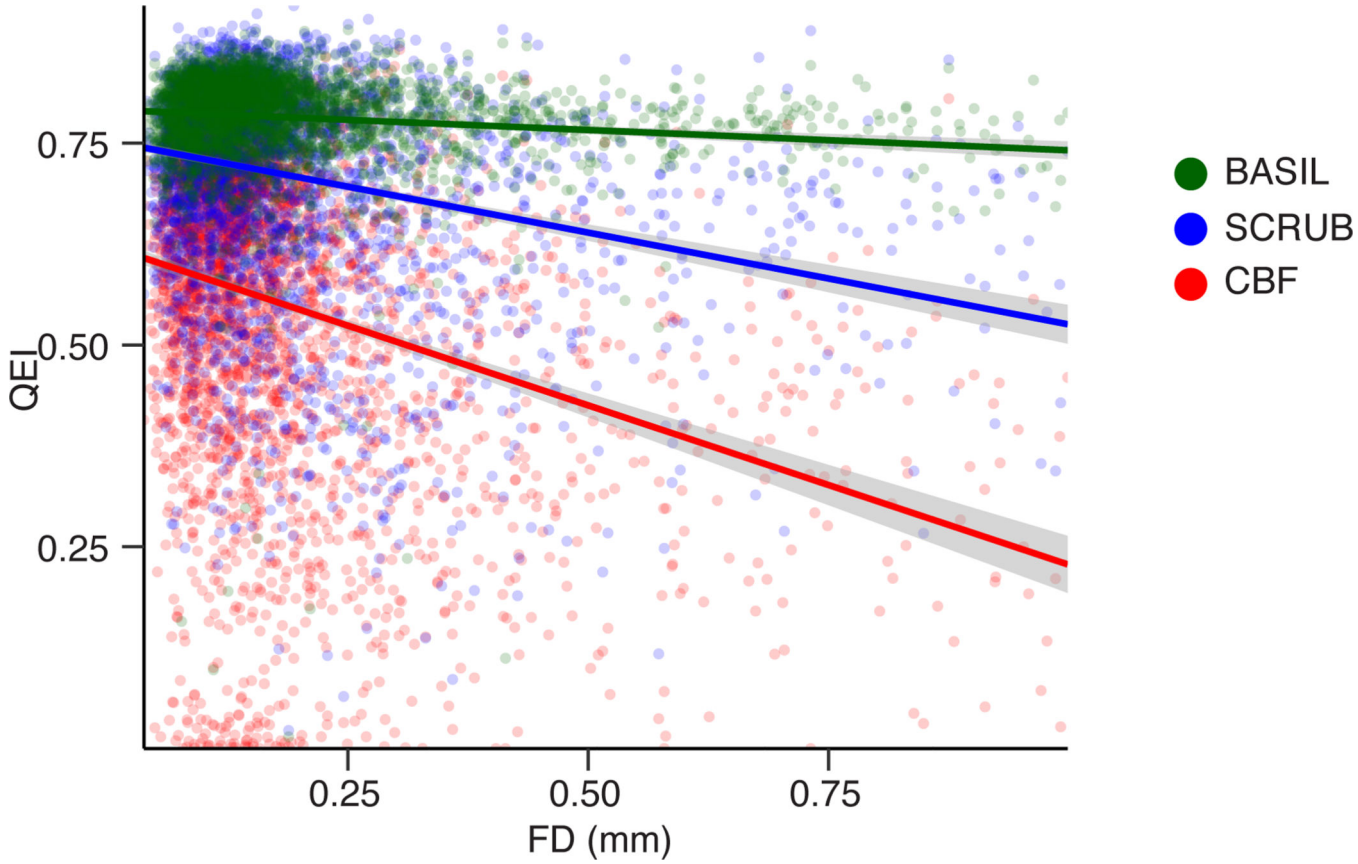

Extended Data Fig. 5. Bayesian methods mitigate impact of in-scanner motion on CBF image quality.

Impact of motion on the CBF image quality as assessed by the Quality Evaluation Index. The impact of motion on quality differed significantly among quantification approaches (linear mixed effects model, $F = 228.09$, $p = 1.0 \times 10^{-25}$). The envelope indicates the 95% confidence interval.

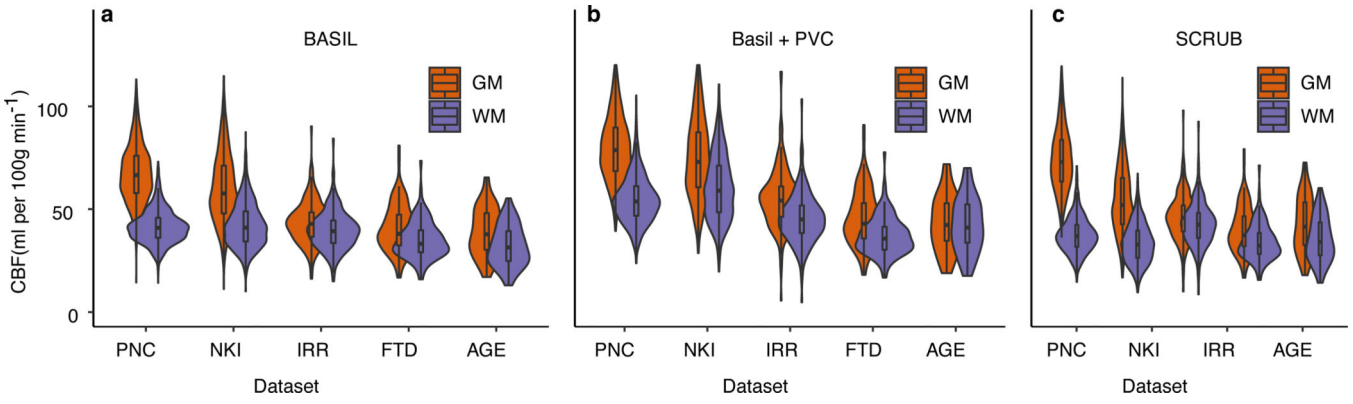

Extended Data Fig. 6. CBF of gray and white matter across datasets.

The distribution of cerebral blood flow (CBF) within grey matter (GM) and white matter (WM) is displayed for each dataset, for each quantification option: the standard CBF model, BASIL (**a**), BASIL with partial volume correction (PVC; **b**), and SCRUB (**c**). SCRUB could

not be applied for the FTD dataset as an ASL timeseries is required; the sequence used for that study provided only a single ΔM image. Boxes within each violin plot indicate interquartile range with the median shown as a white dot.

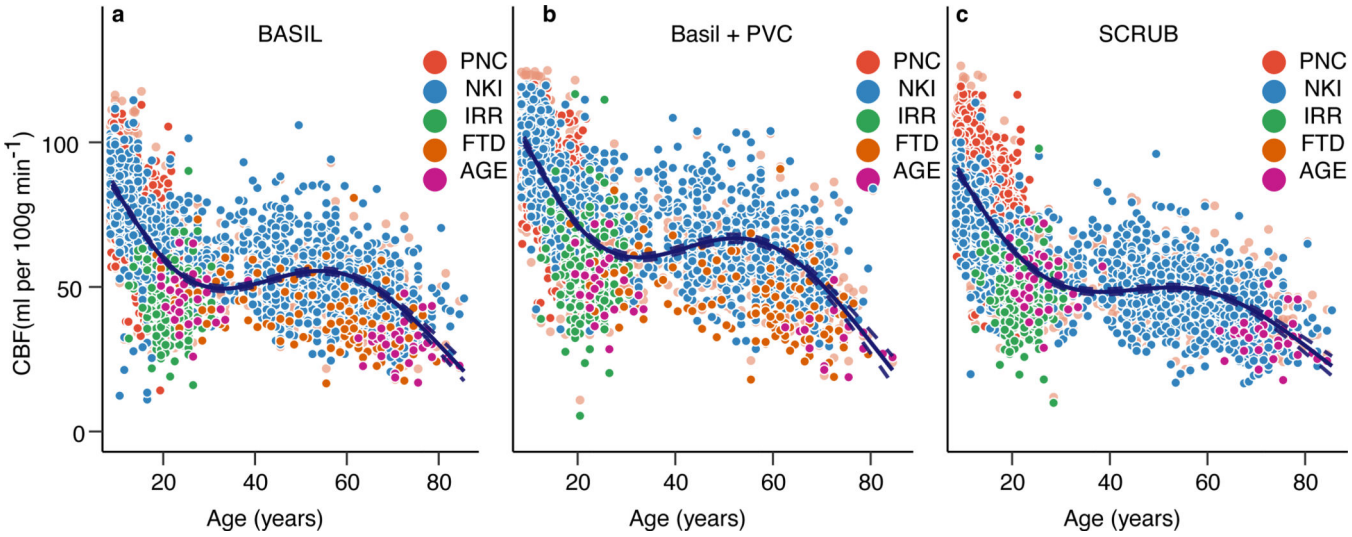

Extended Data Fig. 7. CBF declines nonlinearly with age over the lifespan.

Evolution of gray matter CBF with age over the lifespan across all five datasets. For each dataset, we used four methods for quantifying CBF: the standard CBF model (see main text), BASIL (**a**), BASIL with partial volume correction (PVC; **b**), and SCRUB (**c**). We used a generalized additive model with penalized splines to characterize the nonlinear evolution of CBF over age. The thick black line represents the predicted values, while the dashed lines represent the 95% confidence intervals.

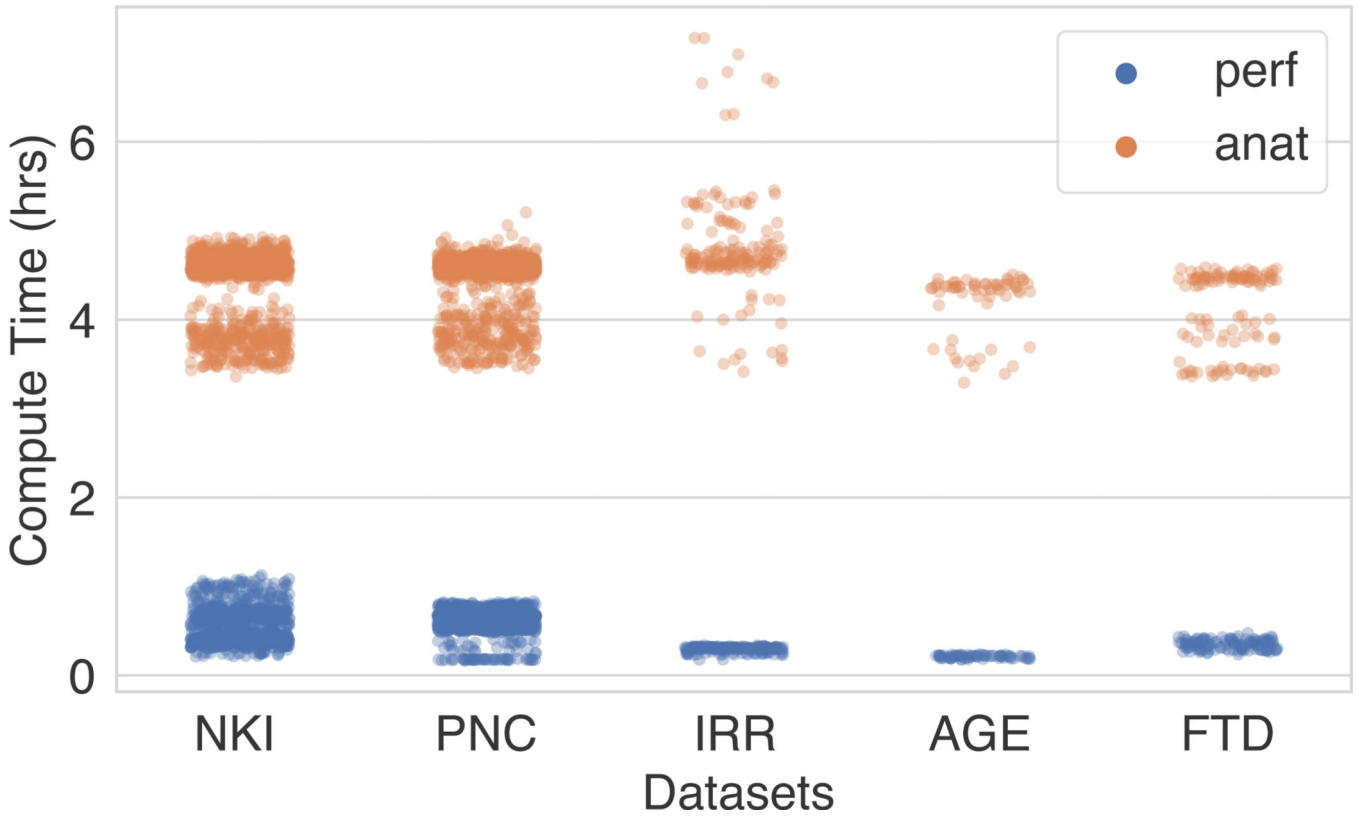

Extended Data Fig. 8. Compute time for ASLPrep.

Distribution of compute time for each dataset, separated by ASL processing and anatomic processing (which relies upon sMRIPrep). Anatomic preprocessing always required a longer duration, with ASL preprocessing and CBF computation requiring less than 70 minutes in all datasets.

Supplementary Material

Refer to Web version on PubMed Central for supplementary material.

Acknowledgements

We acknowledge the support of the following grants: nos. RF1MH121867 (O.E., R.A.P., T.D.S., M.M.), R01MH120482 (T.D.S. and M.M.), R01EB022573 (C.D. and T.D.S.), F31MH126569 (D.Z.), R01MH123550 (T.D.S.), T32MH019112 (E.B.B. and R.E.G.), R01MH120811 (D.J.O.), R01MH112847 (T.D.S.), R01MH112070 (C.D.), RF1AG054409 (C.D.), U01AG052943 (C.M.), U19AG063911 (B.B. and H.R.), AG062422 (H.R.), AG045333 (H.R.), AG019724 (H.R.), P01AG066597 (C.M.), P41EB015893 (J.A.D.), R01MH111886 (D.J.O.), R01MH119219 (R.E.G. and R.C.G.), R01AG054519 (J.S.P.), K01AG061277 (J.S.P.), R01MH120174 (D.R.R.), R01MH119185 (D.R.R.), R03AG063213 (S.D.), R01NS111115 and P30AG072979 (J.A.D.), and the Swiss National Science Foundation Ambizione 185872 (O.E.). Support was provided by the Dutch Heart Foundation (2020T049; H.J.M.M.M.), by the Eurostars-2 joint program (H.J.M.M.M.) with cofunding from the European Union Horizon 2020 research and innovation program (ASPIRE E!113701) provided by the Netherlands Enterprise Agency (RvO), the EU Joint Program for Neurodegenerative Disease Research provided by the Netherlands Organization for health Research and Development and Alzheimer Nederland (DEBBIE JPND2020-568-106; H.J.M.M.M.), and the AE foundation (T.D.S.). Additional support was provided by the Center for Biomedical Image Computing and Analytics (CBICA; A.A., M.C., T.D.S. and C.D.) the Penn-CHOP Lifespan Brain Institute (LiBI; T.D.S., R.C.G. and R.E.G.).

References

1. Herculano-Houzel S. The remarkable, yet not extraordinary, human brain as a scaled-up primate brain and its associated cost. Proc. Natl Acad. Sci. USA 109, 10661–10668 (2012). [PubMed: 22723358]
2. Dolui S, Li Z, Nasrallah IM, Detre JA & Wolk DA Arterial spin labeling versus 18F-FDG-PET to identify mild cognitive impairment. NeuroImage Clin. 25, 102146 (2020). [PubMed: 31931403]
3. Satterthwaite TD et al. Impact of puberty on the evolution of cerebral perfusion during adolescence. Proc. Natl Acad. Sci. USA 111, 8643–8648 (2014). [PubMed: 24912164]
4. Hays CC, Zlatar ZZ & Wierenga CE The utility of cerebral blood flow as a biomarker of preclinical Alzheimer's disease. Cell. Mol. Neurobiol 36, 167–179 (2016). [PubMed: 26898552]
5. Alsop DC et al. Recommended implementation of arterial spin labeled perfusion MRI for clinical applications: a consensus of the ISMRM Perfusion Study Group and the European Consortium for ASL in dementia. Magn. Reson. Med. 73, 102–116 (2015). [PubMed: 24715426]
6. Borogovac A. & Asllani I. Arterial spin labeling (ASL) fMRI: advantages, theoretical constrains and experimental challenges in neurosciences. Int. J. Biomed. Imag. https://www.hindawi.com/journals/ijbi/2012/818456/ (2012).
7. Gorgolewski KJ et al. The brain imaging data structure, a format for organizing and describing outputs of neuroimaging experiments. Sci. Data 3, 160044 (2016). [PubMed: 27326542]
8. Esteban O. et al. fMRIPrep: a robust preprocessing pipeline for functional MRI. Nat. Methods 16, 111–116 (2019). [PubMed: 30532080]
9. Jenkinson M, Beckmann CF, Behrens TEJ, Woolrich MW & Smith SM FSL. NeuroImage 62, 782–790 (2012). [PubMed: 21979382]
10. Fischl B. FreeSurfer. NeuroImage 62, 774–781 (2012). [PubMed: 22248573]
11. Cox RW & Hyde JS Software tools for analysis and visualization of fMRI data. NMR Biomed. 10, 171–178 (1997). [PubMed: 9430344]
12. Avants BB et al. A reproducible evaluation of ANTs similarity metric performance in brain image registration. NeuroImage 54, 2033–2044 (2011). [PubMed: 20851191]
13. Esteban O, Markiewicz CJ, Blair R, Poldrack RA & Gorgolewski KJ sMRIPrep: structural MRI PREProcessing workflows. Zenodo 10.5281/zenodo.4313270 (2020).
14. Esteban O. et al. The Bermuda Triangle of dand f-MRI sailors software for susceptibility distortions (SDCFlows). Preprint at 10.31219/osf.io/gy8nt (2021).
15. Dolui S. et al. Structural Correlation-based Outlier Rejection (SCORE) algorithm for arterial spin labeling time series: SCORE: denoising algorithm for ASL. J. Magn. Reson. Imaging 45, 1786–1797 (2017). [PubMed: 27570967]
16. Buxton RB et al. A general kinetic model for quantitative perfusion imaging with arterial spin labeling. Magn. Reson. Med 40, 383–396 (1998). [PubMed: 9727941]
17. Chappell MA, Groves AR, Whitcher B. & Woolrich MW Variational Bayesian inference for a nonlinear forward model. IEEE Trans. Signal Process. 57, 223–236 (2009).
18. Dolui S. SCRUB: a structural correlation and empirical robust Bayesian method for ASL data. In Proc. International Society for Magnetic Resonance in Medicine, Singapore, May http://archive.ismrm.org/2016/2880.html (ISMRM, 2016).
19. Gorgolewski K. et al. Nipype: a flexible, lightweight and extensible neuroimaging data processing framework in Python. Front. Neuroinform 10.3389/fninf.2011.00013 (2011).
20. Wood SN Generalized Additive Models: An Introduction with R 2nd edn (CRC Press, 2017).
21. Detre JA, Leigh JS, Williams DS & Koretsky AP Perfusion imaging. Magn. Reson. Med 23, 37–45 (1992). [PubMed: 1734182]
22. Esteban O. et al. NiPreps: enabling the division of labor in neuroimaging beyond fMRIPrep. Preprint at 10.31219/osf.io/ujxp6
23. Gorgolewski KJ et al. BIDS apps: Improving ease of use, accessibility, and reproducibility of neuroimaging data analysis methods. PLoS Comput. Biol 13, e1005209 (2017).
24. Cieslak M. et al. QSIPrep: an integrative platform for preprocessing and reconstructing diffusion MRI data. Nat. Methods 18, 775–778 (2021). [PubMed: 34155395]

25. Tustison NJ et al. N4ITK: improved N3 bias correction. IEEE Trans. Med. Imaging 29, 1310–1320 (2010). [PubMed: 20378467]
26. Reuter M, Rosas HD & Fischl B. Highly accurate inverse consistent registration: a robust approach. NeuroImage 53, 1181–1196 (2010). [PubMed: 20637289]
27. Marcus DS et al. Open Access Series of Imaging Studies (OASIS): cross-sectional MRI data in young, middle aged, nondemented, and demented older adults. J. Cogn. Neurosci 19, 1498–1507 (2007). [PubMed: 17714011]
28. Nooner KB et al. The NKI-Rockland sample: a model for accelerating the pace of discovery science in psychiatry. Front. Neurosci 6, 152 (2012). [PubMed: 23087608]
29. Zhang Y, Brady M. & Smith S. Segmentation of brain MR images through a hidden Markov random field model and the expectation-maximization algorithm. IEEE Trans. Med. Imaging 20, 45–57 (2001). [PubMed: 11293691]
30. Fonov V, Evans A, McKinstry R, Almli C. & Collins D. Unbiased nonlinear average age-appropriate brain templates from birth to adulthood. NeuroImage 47, S102 (2009).
31. Ciric R. et al. TemplateFlow: a community archive of imaging templates and atlases for improved consistency in neuroimaging. Preprint at bioRxiv 10.1101/2021.02.10.430678 (2021).
32. Avants BB, Epstein CL, Grossman M. & Gee JC Symmetric diffeomorphic image registration with cross-correlation: evaluating automated labeling of elderly and neurodegenerative brain. Med. Image Anal 12, 26–41 (2008). [PubMed: 17659998]
33. Satterthwaite TD et al. The Philadelphia Neurodevelopmental Cohort: a publicly available resource for the study of normal and abnormal brain development in youth. NeuroImage 124, 1115–1119 (2016). [PubMed: 25840117]
34. Ferré J-C et al. Arterial spin labeling (ASL) perfusion: techniques and clinical use. Diagn. Interv. Imaging 94, 1211–1223 (2013). [PubMed: 23850321]
35. Jenkinson M. Fast, automated, *N*-dimensional phase-unwrapping algorithm. Magn. Reson. Med 49, 193–197 (2003). [PubMed: 12509838]
36. Jenkinson M, Bannister P, Brady M. & Smith S. Improved optimization for the robust and accurate linear registration and motion correction of brain images. NeuroImage 17, 825–841 (2002). [PubMed: 12377157]
37. Greve DN & Fischl B. Accurate and robust brain image alignment using boundary-based registration. NeuroImage 48, 63–72 (2009). [PubMed: 19573611]
38. Esteban O, Markiewicz CJ, Blair RW, Poldrack RA & Gorgolewski KJ SDCflows: susceptibility distortion correction workflows. Zenodo 10.5281/zenodo.3758524 (2020).
39. Poynton C, Jenkinson M, Whalen S, Golby AJ & Wells W. in Lecture Notes in Computer Science Vol. 5242 (eds Metaxas D. et al.) 271–279 (Springer, 2008).
40. Wong EC, Buxton RB & Frank LR Quantitative imaging of perfusion using a single subtraction (QUIPSS and QUIPSS II). Magn. Reson. Med 39, 702–708 (1998). [PubMed: 9581600]
41. Dai W, Robson PM, Shankaranarayanan A. & Alsop DC Reduced resolution transit delay prescan for quantitative continuous arterial spin labeling perfusion imaging. Magn. Reson. Med 67, 1252–1265 (2012). [PubMed: 22084006]
42. Amukotuwa SA, Yu C. & Zaharchuk G. 3D Pseudocontinuous arterial spin labeling in routine clinical practice: a review of clinically significant artifacts. J. Magn. Reson. Imaging JMRI 43, 11–27 (2016). [PubMed: 25857715]
43. Groves AR, Chappell MA & Woolrich MW Combined spatial and non-spatial prior for inference on MRI time-series. NeuroImage 45, 795–809 (2009). [PubMed: 19162204]
44. Chappell MA et al. Partial volume correction of multiple inversion time arterial spin labeling MRI data. Magn. Reson. Med 65, 1173–1183 (2011). [PubMed: 21337417]
45. Satterthwaite TD et al. An improved framework for confound regression and filtering for control of motion artifact in the preprocessing of resting-state functional connectivity data. NeuroImage 64, 240–256 (2013). [PubMed: 22926292]
46. Power JD, Barnes KA, Snyder AZ, Schlaggar BL & Petersen SE Spurious but systematic correlations in functional connectivity MRI networks arise from subject motion. Neuroimage 59, 2142–2154 (2012). [PubMed: 22019881]

47. Dolui S, Wolf R, Nabavizadeh S, Wolk D. & Detre J. Automated quality evaluation index for 2D ASL CBF maps. In Proc. Int. Soc. Mag. Res. Med. 25 (ISMRM, 2017).

48. Desikan RS et al. An automated labeling system for subdividing the human cerebral cortex on MRI scans into gyral based regions of interest. NeuroImage 31, 968–980 (2006). [PubMed: 16530430]

49. Schaefer A. et al. Local-global parcellation of the human cerebral cortex from intrinsic functional connectivity MRI. Cereb. Cortex 28, 3095–3114 (2018). [PubMed: 28981612]

50. Adebimpe A. et al. PennLINC/aslprep: testing. Zenodo 10.5281/zenodo.4277859 (2020).

51. Chappell MA et al. Partial volume correction in arterial spin labeling perfusion MRI: a method to disentangle anatomy from physiology or an analysis step too far? NeuroImage 238, 118236 (2021). [PubMed: 34091034]

52. Kaczkurkin AN et al. Common and dissociable regional cerebral blood flow differences associate with dimensions of psychopathology across categorical diagnoses. Mol. Psychiatry 23, 1981–1989 (2018). [PubMed: 28924181]

53. Ye FQ et al. H215O PET validation of steady-state arterial spin tagging cerebral blood flow measurements in humans. Magn. Reson. Med 44, 450–456 (2000). [PubMed: 10975898]

54. Burt JB, Helmer M, Shinn M, Anticevic A. & Murray JD Generative modeling of brain maps with spatial autocorrelation. NeuroImage 220, 117038 (2020).

55. Adebimpe A. et al. ASLPrep: a platform for processing of arterial spin labeled MRI and quantification of regional brain perfusion. Zenodo 10.5281/zenodo.4815777 (2022).

56. Adebimpe A. et al. ASLPrep: a platform for processing of arterial spin labeled MRI and quantification of regional brain perfusion. Code Ocean https://codeocean.com/capsule/9217309/tree/v1 (2022).

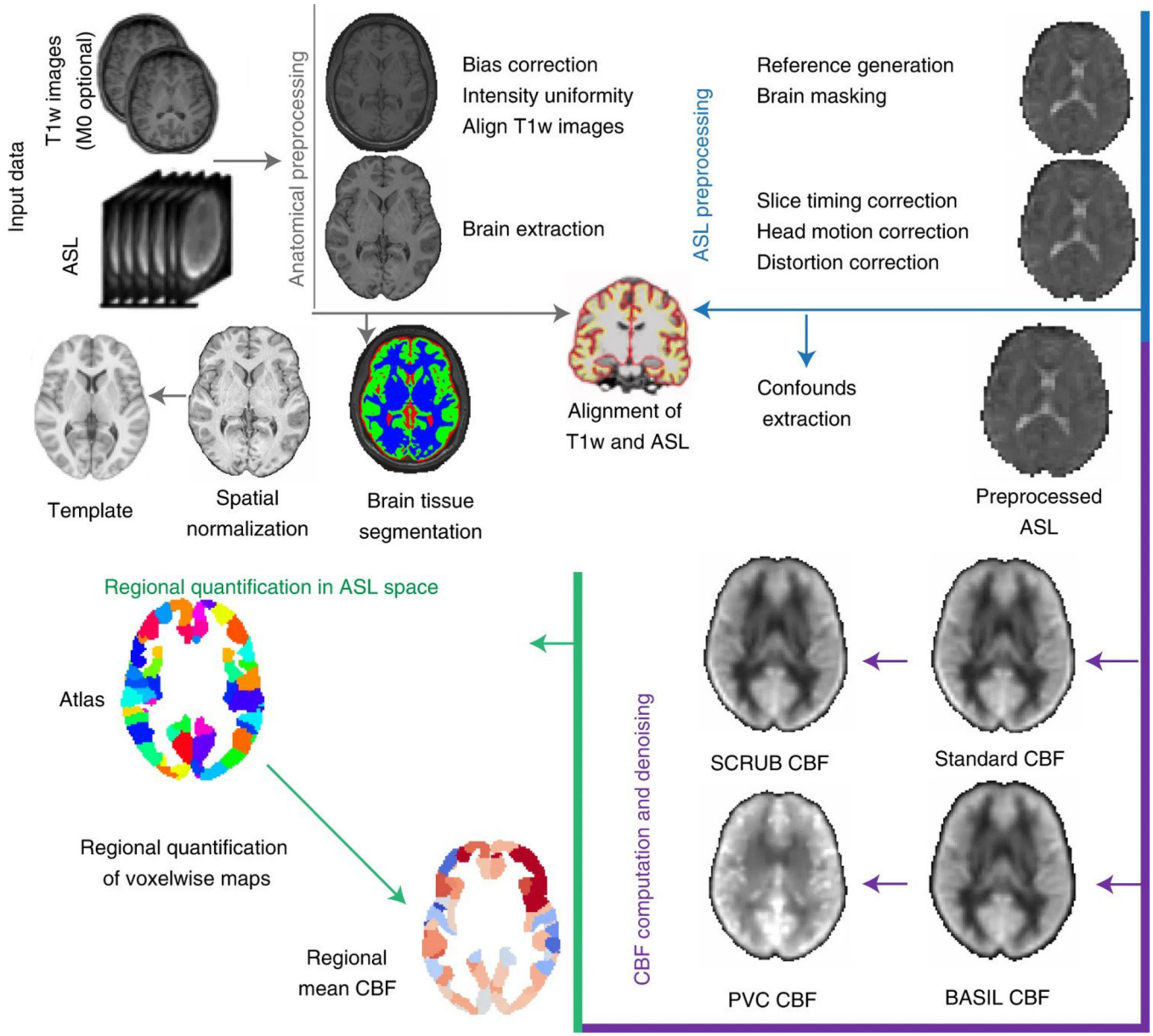

Fig. 1: Overview of ASLPrep.

Input data to ASLPrep includes ASL images, anatomical (T1 weighted) images and (optionally) M0 reference images. Anatomical preprocessing is executed using standard tools (as implemented in sMRIPrep); ASL image processing includes both preprocessing and CBF computation.

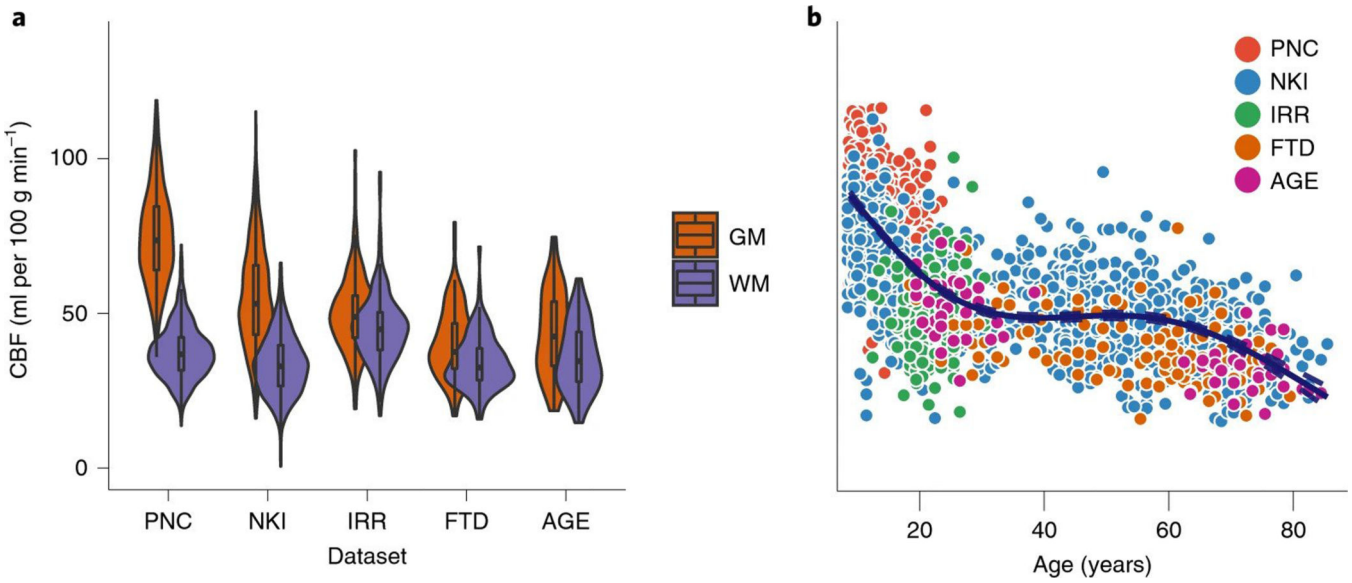

Fig. 2: ASLPrep quantifies CBF across sequences, scanners and the lifespan.

a, CBF in GM and WM for each dataset. Boxes in each violin plot indicate interquartile range with the median shown as a white dot. **b**, GM CBF across the lifespan. The thick black line represents the predicted values from a generalized additive model; the dashed lines indicate the 95% confidence interval ($R^2 = 0.57$; $P = 1.1 \times 10^{-16}$).